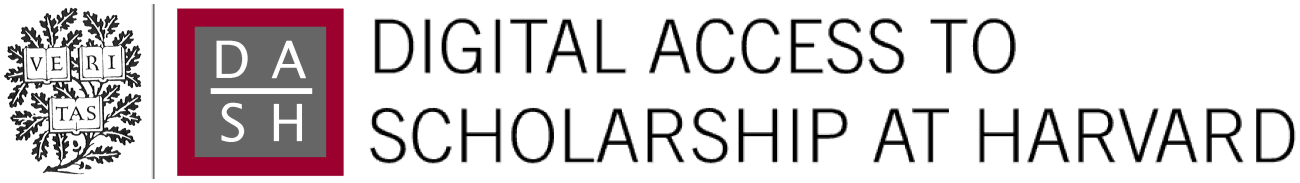

An Embryonic Stem Cell-Based System for Rapid Analysis of Transcriptional Enhancers

An Embryonic Stem Cell Based System for Rapid Analysis of Transcriptional Enhancers

Kaloyan M. Tsanov[1,2], Yuichi Nishi[1], Kevin A. Peterson[1], Jing Liu[1,3], Manfred Baetscher[2,3] and Andrew P. McMahon[1,2,3*]

[1]Department of Stem Cell and Regenerative Biology, Harvard University, Cambridge, Massachusetts

[2]Department of Molecular and Cellular Biology, Harvard University, Cambridge, Massachusetts

[3]Harvard Stem Cell Institute, Cambridge, Massachusetts

*Correspondence: Andrew P. McMahon, Department of Stem Cell and Regenerative Biology, SF358A, Harvard University, 7 Divinity Avenue, Cambridge MA, 02138; Phone: (617) 496-3757; Fax: (617) 496-3763; E-mail: mcmahon@mcb.harvard.edu

Running Head: ESC based system for rapid enhancer analysis

Keywords: embryonic stem cells; gene targeting; enhancer elements; transcription; gene regulatory networks

Grant Sponsor: NIH, Grant number: R37 NS033642 (to A.P.M.)

Abstract

With the growing use of genome-wide screens for *cis*-regulatory elements, there is a pressing need for platforms that enable fast and cost-effective experimental validation of identified hits in relevant developmental and tissue contexts. Here, we describe a murine embryonic stem cell (ESC) based system that facilitates rapid analysis of putative transcriptional enhancers. Candidate enhancers are targeted with high efficiency to a defined genomic locus via recombinase-mediated cassette exchange (RMCE). Targeted ESCs are subsequently differentiated *in vitro* into desired cell types, where enhancer activity is monitored by reporter gene expression. As a proof of principle, we analyzed a previously characterized, Sonic hedgehog (Shh)-dependent, V3 interneuron progenitor (pV3)-specific enhancer for the *Nkx2.2* gene, and observed highly specific enhancer activity. Given the broad potential of ESCs to generate a spectrum of cell types, this system can serve as an effective platform for the characterization of gene regulatory networks controlling cell fate specification and cell function.

Enhancers are *cis*-regulatory DNA elements that modulate transcription independent of their position and orientation with respect to the transcriptional start site (Banerji *et al.*, 1981). A given enhancer contains binding sites for different transcription factors; the specific combination of DNA-protein interactions determines whether the enhancer is active or silent, ensuring appropriate spatial and temporal activity of target genes. As key regulators of gene expression, enhancers play critical roles in development, disease, and evolution (Ben-Tabou de-Leon and Davidson, 2007; Visel *et al.*, 2009b). Consequently, a systematic comprehensive decoding of their regulatory actions is an important goal, and especially so for the understanding of how cell fates are determined on differentiation of stem cells.

The advent of powerful genomic technologies has allowed for the unprecedented genome-wide prediction of enhancer elements (Rada-Iglesias *et al.*, 2011; Visel *et al.*, 2009a). However, to rapidly validate and characterize the vast number of genomic regions with regulatory potential remains a considerable challenge, particularly in mammals. In a typical enhancer assay, a putative enhancer element is placed upstream of a minimal promoter driving a reporter gene whose expression is analyzed in an appropriate experimental system (Loots, 2008). There are significant drawbacks associated with many of the existing methodologies. For example, transient transfections of reporter constructs are easy to perform but assess the elements in multiple copies and in a non-chromosomal context. At the other end of the spectrum, mouse transgenesis offers a more natural *in vivo* context, yet it is expensive, time-consuming, and laborious. This is further aggravated by the fact that the copy number and integration sites of reporter constructs cannot be controlled, thus necessitating the analysis of multiple lines per element to control for position effects at the site of integration and copy number differences that

confound analysis. Given these and other constraints, it is critical to develop faster, scalable, and more cost-effective experimental systems that replicate normal regulatory mechanisms.

Embryonic stem cells (ESCs) are well suited for this purpose, since they are amenable to controlled genetic manipulations (Capecchi, 1989; Turan *et al.*, 2011) and can be differentiated into a variety of cell lineages closely replicating the normal programs of cell fate specification (Keller, 2005). The general utility of ESC based approaches for analysis of *cis*-regulatory elements has been shown (Xian *et al.*, 2005; Zhang *et al.*, 2008). However, a high-throughput application requires the development of an efficient, reproducible and rapid strategy that enables position-independent activity of potentially any enhancer of interest. To these ends, we developed a novel system that enables reproducible targeting of candidate enhancers through recombinase-mediated cassette exchange (RMCE) at the *Gt(ROSA)26Sor* locus (hereafter referred to as the *Rosa26* locus) (Turan *et al.*, 2011; Zambrowicz *et al.*, 1997). The *Rosa26* locus is a transcriptionally permissive environment and eliminates potential position effects associated with random integration (Zambrowicz *et al.*, 1997). Targeted ESCs can be assayed directly or differentiated into various cell types to assess tissue-specific enhancer activity. As a proof of principle, we generated neuralized embryoid bodies (EBs) from ESCs and analyzed Sonic hedgehog (Shh)-mediated activation of the *Nkx2.2* gene in V3 interneuron progenitors (pV3) (Briscoe *et al.*, 1999). We selected a pV3-specific enhancer of *Nkx2.2* that has previously been characterized in transgenic mice and shown to be dependent upon a single Gli transcription factor binding site (Lei *et al.*, 2006; Vokes *et al.*, 2007). Characterization of this enhancer *in vitro* recapitulates the *in vivo* analysis, validating our enhancer analysis platform. In addition, we demonstrate how the system can be further optimized to improve its capability for high-throughput applications.

To allow for high-throughput analysis of putative enhancers, we took advantage of the high efficiency of RMCE and selected the *Rosa26* locus as a target site, as its activity in most cell types indicates a chromatin configuration that is predicted to permit normal, position-independent regulation of test enhancers (Zambrowicz *et al.*, 1997). To facilitate RMCE, we targeted a FLPo recombinase expression cassette, flanked by F3 and FRT recognition sites, to the *Rosa26* locus (cell line Rosa26 (FLPo)) (Fig. 1a). This configuration allows for high recombination efficiency, prevents internal recombination, and provides an endogenous source of recombinase activity that is conveniently self-terminated upon recombination (Raymond and Soriano, 2007; Seibler and Bode, 1997; Seibler *et al.*, 2005). To prevent random integration and achieve stringent selection of correctly targeted clones, we used a neomycin resistance gene (Neo) that lacks a promoter and an ATG translation start codon (Fig. 1b). Only upon successful recombination, a splice acceptor and ATG codon engineered in the Rosa26 (FLPo) line allow for Neo expression from the endogenous *Rosa26* promoter (Beard *et al.*, 2006). Indeed, we observed 98% selection efficiency (48/49 recombinant colonies), in line with similar targeting strategies (Seibler *et al.*, 2005; Wang *et al.*, 2007) (Fig. 1c and data not shown). A correctly integrated enhancer-reporter cassette was flanked by single copies of the full-length chicken β-globin insulator to block local influences on enhancer activity (Burgess-Beusse *et al.*, 2002; Chung *et al.*, 1997). Together, all these features enable a highly efficient analysis, where the need to screen dozens of colonies for correct integration and assess multiple clones per construct due to position effects is eliminated.

Once we optimized the parameters for consistent targeting results, we explored a number of protocol modifications to improve the scalability of the approach (Table 1). On average, at least one recombinant colony per million electroporated cells was obtained consistently under all

conditions tested. As a result, we have adapted our system to a 6-well-plate format, allowing for moderate-throughput applications. Additional optimization, such as testing the use of even fewer cells per electroporation or lipofection-based delivery methods, may improve on targeting efficiency with regard to the number of input cells.

Next, we validated our platform for enhancer analysis (schematized in Fig. 2). A 420-bp enhancer located 1.7 kb upstream of the *Nkx2.2* coding sequence recapitulates the pV3-specific *Nkx2.2* expression pattern *in vivo* (Lei *et al.*, 2006). This activity is Shh-dependent; mutation of a unique Gli factor binding site – Gli proteins are the transcriptional effectors of the Shh pathway – abolishes enhancer activity. Rosa26 (FLPo) cells were targeted with this element and subjected to a 5-day EB differentiation protocol that utilizes the neuralizing activity of retinoic acid (RA), in conjunction with a small-molecule agonist of the Shh pathway (SAG), to generate a mix of Shh-dependent neural progenitors that includes *Nkx2.2*$^+$, pV3 cells (Chen *et al.*, 2002; Wichterle *et al.*, 2002). As expected, nearly all *Nkx2.2*$^+$ cells co-expressed the β-gal reporter (91.1 ± 1.7%) (Fig. 3i-l, q; data from two independent clones). We did detect a population of β-gal single-positive cells (20.6 ± 3.0% of all β-gal$^+$ cells), consistent with *in vivo* observations (Lei *et al.*, 2006). This likely reflects the absence of sequences that refine *Nkx2.2* expression after Shh activation, notably those that suppress activity in the floor plate. Importantly, enhancer activity was Shh-dependent. First, omission of the Shh agonist abolished reporter along with *Nkx2.2* expression (2.4 ± 1.1% β-gal$^+$ cells) (Fig. 3e-h, r). Further, a mutation of the critical Gli binding site similarly abrogated reporter expression (1.8 ± 0.6% β-gal$^+$ cells) (Fig. 3m-p, q, r). An enhancer-less reporter showed minimal levels of reporter activation (1.6 ± 0.4% β-gal$^+$ cells) despite appropriate derivation of V3 progenitors (25.9 ± 4.2% *Nkx2.2*$^+$ cells), indicating that promoter background is negligible and does not influence the analysis (Fig. 3a-d, q, r).

Collectively, these data demonstrate that transcriptional activity of the enhancer element can be reliably analyzed in this *in vitro* system.

We also developed an exchange vector with a nuclear *lacZ::GFP* fusion reporter to simplify scoring of nuclear signals. Using this modified construct, we obtained essentially identical results (91.2 ± 1.5% *Nkx2.2*$^{+}$ cells co-expressed reporter for the wild-type enhancer; 15.5 ± 2.3% reporter cells were single-positive) (Supp. Fig. 1). Besides facilitating scoring of immunostained samples, this reporter also enables potential FACS analysis with the GFP marker as an additional means of quantitatively assessing enhancer activity.

In conclusion, we have developed a novel murine ESC based system for fast, scalable, and cost-effective analysis of putative transcriptional enhancers. Our methodology can be applied to other neural and non-neural enhancers, given the broad array of cell types that can be generated from ESCs (Keller, 2005), and potentially to human ESCs, since protocols for their genetic manipulation and directed differentiation are available (Hockemeyer and Jaenisch, 2010; Irion *et al.*, 2008). The same general strategy can also be implemented for the analysis of other types of *cis*-regulatory elements, such as silencers or insulators. Thus, our system provides a versatile tool that could find broad application in large-scale studies of the transcriptional gene regulation in ESCs or diverse developmental and tissue contexts.

Methods

Plasmid construction

To construct the *Rosa26* targeting vector (pRosa-17), a PGK-Neo-3xpA cassette was replaced with ATG-F3-PGK-Puro-pA and PGK-FLPo-pA cassettes in the pBigT vector (Srinivas *et al.*,

2001). The former fragment was PCR amplified from the pPGKpuro vector (Tucker *et al.*, 1996) (ATG and F3 sequences were included in the primer tails), and the latter obtained by excision from the pPGKFLPobpA vector (Raymond and Soriano, 2007). Next, an FRT-1xIns fragment was PCR amplified from the pHSP68lacZ2XINS vector (Vokes *et al.*, 2007) (FRT sequence was included in the primer tail), inserted downstream of FLPo-pA to replace a pA sequence in the pBigT backbone, and the entire ATG-to-1xIns fragment cloned into pRosaPAS (Mao *et al.*, 2005).

To construct the exchange vector (pXCHG3), an F3-ΔATGNeo-pA-3xpA cassette was PCR amplified from pBigT (Srinivas *et al.*, 2001) (ATG was excluded and F3 sequence included in the primer tails), and an FRT site generated by annealing of pre-synthesized oligonucleotides (IDT). The two fragments were ligated and inserted downstream of a pA sequence cloned from pPGKFLPobpA (Raymond and Soriano, 2007) in pBlueScript (Stratagene)**.** A 1xIns-hsp68-lacZ-pA cassette (Vokes *et al.*, 2007) was cloned immediately upstream of the FRT site. F3 and FRT sequences used in all vectors were respectively: GAAGTTCCTATTCCGAAGTTCCTATTCTT-CAAATAGTATAGGAACTTC and GAAGTTCCTATACTTTCTAGAGAATAGGAACTTCG-GAATAGGAACTTC. *Nkx2.2* enhancer variants were subsequently inserted at a unique KpnI site upstream of the hsp68 promoter. The Nkx2.2-420bp and Nkx2.2-GliM constructs were generated as previously described (Lei *et al.*, 2006).

To generate the modified exchange vector (pXCHG-IHZG), 1xIns and hsp68 sequences were PCR amplified from pHSP68lacZ2XINS (Vokes *et al.*, 2007), and cloned into the pBlueScript-KS(+) vector (Stratagene) to generate pBS-Ins-Hsp68. Next, the lacZ coding sequence was PCR amplified from pHSP68lacZ2XINS (Vokes *et al.*, 2007), and a 3X-NLS-GFP-pA fragment PCR amplified from pCIG (Megason and McMahon, 2002). The two

fragments were cloned into pBS-Ins-Hsp68 to generate pBS-1xIns-hsp68-lacZ-3XNLS-GFP-pA (pIHZG). An attR1-attR2 Gateway® selection cassette (Invitrogen) was inserted immediately upstream of hsp68, and the entire 1xIns-to-pA fragment used to replace 1xIns-hsp68-lacZ-pA in pXCHG3. The Nkx2.2-420bp enhancer was cloned into the pENTR1A vector (Invitrogen) and inserted in pXCHG-IHZG via Gateway® LR recombination, as per manufacturer's protocol (Invitrogen).

For the optimization experiments, a pCAGGS-FLPo expression vector was constructed by cloning the FLPo coding sequence (Raymond and Soriano, 2007) downstream of the CAGGS promoter of pCIG (Megason and McMahon, 2002).

Gene targeting

For generation of the Rosa26 (FLPo) line, 20 μg targeting vector was linearized with SwaI, phenol/chloroform purified, and added to 10^7 V6.5 cells (Eggan *et al.*, 2001) in 800 μl cold PBS. Cells were electroporated at 230 V and 500 μF using Gene Pulser (BioRad), and plated onto 10-cm dishes with puromycin-resistant MEFs. 3 μg/μl puromycin (Sigma) was added on the following day, medium was changed daily, and colonies were picked after 6 days of selection, as described previously (Hogan *et al.*, 1994). Picked clones were expanded in 96-well plates with MEF feeders. Properly targeted clones were identified by junction PCR, expanded, and stocked. Primer sequences for genotyping were as follows: for 5' end, CCGCCTAAAGAAGAGGCTGT-GCTTTGG (Rosa05) and CAAGGAAACCCTGGACTACTGCGCCC (Rosa15); for 3' end, CTGGGCTGCTGGTTGATGACCCTGC (Rosa02) and GGGCAATCTGGGAAGGTTCCTTA-AGAA (Rosa11).

For RMCE, 20 μg circular exchange vector was added to 6 x 10^6 Rosa26 (FLPo) cells in 800 μl cold PBS. Cells were electroporated at 240 V and 500 μF using Gene Pulser (BioRad), and plated onto 10-cm dishes with neomycin-resistant MEFs. For 6-well-plate format, the same conditions were used, except that 4 x 10^6 cells were electroporated and 1.5 x 10^6 cells plated per well in 6-well plates. 300 μg/ml G418 (Geneticin®; Invitrogen) was added on the following day and medium was changed daily. Colonies were picked 6 days after the onset of selection, expanded in 48-well plates with MEF feeders, and cultured in complete medium containing 200 μg/ml G418. Appropriate recombination events were identified by junction PCR, targeted cells were expanded, and frozen stocks prepared. Primer sequences for genotyping were as follows: for 5'end, CTCTGAGTTGTTATCAGTAAGGGAGC (Xchg01) and GATTGTCTGTTGTGC-CCAGTCATAG (Xchg11); for 3' end, GTCGCTACCATTACCAGTTGGTCT (Xchg02) and CCCAGATGACTCCTATCCTCCATTT (Xchg12). PCR conditions were as follows: 94ºC for 2 min; 35 cycles of 94ºC for 10 s, 55ºC for 30 s, 68ºC for 1 min (5' end) or 2 min (3' end); 68ºC for 5 min. The Taq PCR Core Kit was used following manufacturer's protocol (Qiagen).

For testing different targeting conditions, a given parameter was modified and the effect of the modification on the yield of recombinant colonies determined as indicated in Table 1. When exogenous FLPo was provided, this was achieved by co-electroporation with 20 μg pCAGGS-FLPo. Each condition was repeated in at least three replicates and data on colony yield are presented as mean ± SEM, with the exceptions noted in Table 1.

ESC culture and directed differentiation

All ESC lines were maintained using standard procedures, in complete ESC medium containing 15% fetal bovine serum (FBS; Hyclone) and 1,000 units/ml recombinant leukemia inhibitory

factor (LIF; Chemicon) (Hogan *et al.*, 1994). Directed differentiation followed published procedures (Wichterle *et al.*, 2002). Two days after EB formation, medium was replaced and supplemented with 500 nM retinoic acid (RA; Sigma) and, where applicable, 1 μM of the Shh-agonist, SAG (Alexis Biochemicals). EBs were cultured for additional 3 days to induce neural progenitor stages, at which point they were harvested, fixed, sectioned and processed for immunostaining, as described previously (Wichterle *et al.*, 2002).

Immunocytochemistry and quantification

Primary antibodies were as follows: rabbit anti-β-galactosidase (1:40,000, Cappel), and mouse anti-Nkx2.2 (1:20, Developmental Studies Hybridoma Bank). Secondary antibodies were appropriately-conjugated IgG (H+L) Alexa Fluor® 488 or 568 (1: 500, Invitrogen). Stained sections were imaged on a LSM510/710 META confocal microscope (Zeiss). To quantify co-expression, β-gal and *Nkx2.2* immunoreactivity was quantified by individual cell counts, and the overlap determined relative to the number of *Nkx2.2*$^+$ cells. To calculate the proportion of β-gal single-positive cells, the latter were counted and represented as a percentage of all β-gal$^+$ cells. To calculate the total proportion of β-gal$^+$ or *Nkx2.2*$^+$ cells, the respective cells were counted and represented as a percentage of Hoechst-positive cells. In all cases, regions corresponding to fields of view (40X magnification) of at least five different EBs (three for total counts and no-SAG controls) were scored for each sample. Data are presented as mean ± SEM. Differences between samples were compared by one-way ANOVA, where statistical significance is defined as $P < 0.05$.

Acknowledgements

We thank the staff at the Harvard Stem Cell Institute Genome Modification Facility for assistance with the generation of the Rosa26 (FLPo) line, A. Kobayashi, J. McMahon, L. Chen and S. Ohba for technical advice, B. Allen for feedback on the draft, and all members of the McMahon laboratory for invaluable help and discussions. K.M.T. was supported by the Harvard College Research Program and the Pechet Family Fund for Undergraduate Research. K.A.P. was supported by an NRSA postdoctoral fellowship (F32 GM087939). Work in A.P.M.'s laboratory was supported by a grant from the NIH (R37 NS033642).

References

Banerji J, Rusconi S, Schaffner W. 1981. Expression of a beta-globin gene is enhanced by remote SV40 DNA sequences. Cell 27: 299-308.

Beard C, Hochedlinger K, Plath K, Wutz A, Jaenisch R. 2006. Efficient method to generate single-copy transgenic mice by site-specific integration in embryonic stem cells. Genesis 44: 23-28.

Ben-Tabou de-Leon S, Davidson EH. 2007. Gene regulation: gene control network in development. Annu Rev Biophys Biomol Struct 36: 191.

Briscoe J, Sussel L, Serup P, Hartigan-O'Connor D, Jessell TM, Rubenstein JL, Ericson J. 1999. Homeobox gene Nkx2.2 and specification of neuronal identity by graded Sonic hedgehog signalling. Nature 398: 622-627.

Burgess-Beusse B, Farrell C, Gaszner M, Litt M, Mutskov V, Recillas-Targa F, Simpson M, West A, Felsenfeld G. 2002. The insulation of genes from external enhancers and silencing chromatin. Proc Natl Acad Sci U S A 99 Suppl 4: 16433-16437.

Capecchi MR. 1989. The new mouse genetics: altering the genome by gene targeting. Trends Genet 5: 70-76.

Chen JK, Taipale J, Young KE, Maiti T, Beachy PA. 2002. Small molecule modulation of Smoothened activity. Proc Natl Acad Sci U S A 99: 14071-14076.

Chung JH, Bell AC, Felsenfeld G. 1997. Characterization of the chicken beta-globin insulator. Proc Natl Acad Sci U S A 94: 575-580.

Davidson EH. 2006. The Regulatory Genome: Gene Regulatory Networks in Development and Evolution. San Diego: Academic Press.

Eggan K, Akutsu H, Loring J, Jackson-Grusby L, Klemm M, Rideout WM, 3rd, Yanagimachi R, Jaenisch R. 2001. Hybrid vigor, fetal overgrowth, and viability of mice derived by nuclear cloning and tetraploid embryo complementation. Proc Natl Acad Sci U S A 98: 6209-6214.

Hockemeyer D, Jaenisch R. 2010. Gene targeting in human pluripotent cells. Cold Spring Harb Symp Quant Biol 75: 201-209.

Hogan B, Beddington R, Costantini F, Lacey E, editors. 1994. Manipulating the Mouse Embryo: A Laboratory Manual, 2nd Edition. Cold Spring Harbor: Cold Spring Harbor Laboratory Press.

Irion S, Nostro MC, Kattman SJ, Keller GM. 2008. Directed differentiation of pluripotent stem cells: from developmental biology to therapeutic applications. Cold Spring Harb Symp Quant Biol 73: 101-110.

Keller G. 2005. Embryonic stem cell differentiation: emergence of a new era in biology and medicine. Genes Dev 19: 1129-1155.

Lei Q, Jeong Y, Misra K, Li S, Zelman AK, Epstein DJ, Matise MP. 2006. Wnt signaling inhibitors regulate the transcriptional response to morphogenetic Shh-Gli signaling in the neural tube. Dev Cell 11: 325-337.

Loots GG. 2008. Genomic identification of regulatory elements by evolutionary sequence comparison and functional analysis. Adv Genet 61: 269-293.

Mao J, Barrow J, McMahon J, Vaughan J, McMahon AP. 2005. An ES cell system for rapid, spatial and temporal analysis of gene function in vitro and in vivo. Nucleic Acids Res 33: e155.

Megason SG, McMahon AP. 2002. A mitogen gradient of dorsal midline Wnts organizes growth in the CNS. Development 129: 2087-2098.

Rada-Iglesias A, Bajpai R, Swigut T, Brugmann SA, Flynn RA, Wysocka J. 2011. A unique chromatin signature uncovers early developmental enhancers in humans. Nature 470: 279-283.

Raymond CS, Soriano P. 2007. High-efficiency FLP and PhiC31 site-specific recombination in mammalian cells. PLoS ONE 2: e162.

Seibler J, Bode J. 1997. Double-reciprocal crossover mediated by FLP-recombinase: a concept and an assay. Biochemistry 36: 1740-1747.

Seibler J, Kuter-Luks B, Kern H, Streu S, Plum L, Mauer J, Kuhn R, Bruning JC, Schwenk F. 2005. Single copy shRNA configuration for ubiquitous gene knockdown in mice. Nucleic Acids Res 33: e67.

Srinivas S, Watanabe T, Lin CS, William CM, Tanabe Y, Jessell TM, Costantini F. 2001. Cre reporter strains produced by targeted insertion of EYFP and ECFP into the ROSA26 locus. BMC Dev Biol 1: 4.

Tucker KL, Beard C, Dausmann J, Jackson-Grusby L, Laird PW, Lei H, Li E, Jaenisch R. 1996. Germ-line passage is required for establishment of methylation and expression patterns of imprinted but not of nonimprinted genes. Genes Dev 10: 1008-1020.

Turan S, Galla M, Ernst E, Qiao J, Voelkel C, Schiedlmeier B, Zehe C, Bode J. 2011. Recombinase-mediated cassette exchange (RMCE): traditional concepts and current challenges. J Mol Biol 407: 193-221.

Visel A, Blow MJ, Li Z, Zhang T, Akiyama JA, Holt A, Plajzer-Frick I, Shoukry M, Wright C, Chen F, Afzal V, Ren B, Rubin EM, Pennacchio LA. 2009a. ChIP-seq accurately predicts tissue-specific activity of enhancers. Nature 457: 854-858.

Visel A, Rubin EM, Pennacchio LA. 2009b. Genomic views of distant-acting enhancers. Nature 461: 199-205.

Vokes SA, Ji H, McCuine S, Tenzen T, Giles S, Zhong S, Longabaugh WJ, Davidson EH, Wong WH, McMahon AP. 2007. Genomic characterization of Gli-activator targets in sonic hedgehog-mediated neural patterning. Development 134: 1977-1989.

Wang J, Theunissen TW, Orkin SH. 2007. Site-directed, virus-free, and inducible RNAi in embryonic stem cells. Proc Natl Acad Sci U S A 104: 20850-20855.

Wichterle H, Lieberam I, Porter JA, Jessell TM. 2002. Directed differentiation of embryonic stem cells into motor neurons. Cell 110: 385-397.

Xian HQ, Werth K, Gottlieb DI. 2005. Promoter analysis in ES cell-derived neural cells. Biochem Biophys Res Commun 327: 155-162.

Zambrowicz BP, Imamoto A, Fiering S, Herzenberg LA, Kerr WG, Soriano P. 1997. Disruption of overlapping transcripts in the ROSA beta geo 26 gene trap strain leads to widespread expression of beta-galactosidase in mouse embryos and hematopoietic cells. Proc Natl Acad Sci U S A 94: 3789-3794.

Zhang X, Horrell SA, Delaney D, Gottlieb DI. 2008. Embryonic stem cells as a platform for analyzing neural gene transcription. Stem Cells 26: 1841-1849.

Figure Legends

Figure 1. Engineering the *Rosa26* locus for RMCE analysis of enhancer activity. (a) Schematic of the strategy to generate the Rosa26 (FLPo) allele. 'X' marks the insertion point within the *Rosa26* locus (genome coordinates chr6:113,026,031 (mm9)). **(b)** Schematic of the RMCE used to target putative enhancers. Gray arrowheads denote primers used for PCR screening for positive clones. **(c)** Representative PCR results from a targeting experiment. The highlighted bands indicate correct integration at the 5' (left) and 3' (right) ends. 1-7, individual clones; NC, negative control (Rosa (FLPo) DNA).

Abbreviations: SA, splice acceptor; ATG, translation initiation codon; F3/FRT, recombination sites; PGK, phosphoglycerokinase promoter; Puro, puromycin resistance gene; pA, polyadenylation/transcription stop signal; FLPo, codon-optimized FLP recombinase; Ins, chicken β-globin insulator; ΔATG-Neo, promoter/ATG-less neomycin resistance gene; Enh, putative enhancer; hsp68, heat shock protein 68 minimal promoter; lacZ, *E. coli* β-galactosidase gene.

Figure 2. Flowchart of the experimental analysis of enhancer activity in neuralized EBs. Putative enhancers (enh) are coupled to the hsp68 minimal promoter driving the expression of a nuclear *lacZ::GFP* reporter (lacZnGFP), and introduced at a defined locus (*Rosa26*) in ESCs via RMCE. Following highly efficient selection for neomycin resistance, successful recombinants are expanded and differentiated *in vitro* to desired cell types, which results in the expression of specific markers (red and orange). Neuralized EB sections are immunostained and analyzed quantitatively to determine overlap between the expression of the reporter gene (green) and an endogenous gene of interest (red). For abbreviations, see Fig. 1. *This time is given for the differentiation protocol used in this study.

Figure 3. Shh-pathway-dependent activation of an *Nkx2.2* enhancer in ESC-derived neural progenitors. (a-d) Neural progenitors harboring an empty exchange vector. Activity of the *Nkx2.2* enhancer (Nkx2.2-420bp) in the absence **(e-h)**, or presence of SAG **(i-l)**; arrowheads in inset (k) point to *Nkx2.2*$^{+}$β-gal^{+} cells. **(m-p)** SAG-treated neural progenitors harboring an *Nkx2.2* enhancer with a mutated Gli binding site (Nkx2.2-GliM). Magnification: 40X. **(q)** Quantification of β-gal/*Nkx2.2* co-expression. **, $P < 0.01$. **(r)** Quantification of *Nkx2.2* (purple) and β-gal (blue) expression.

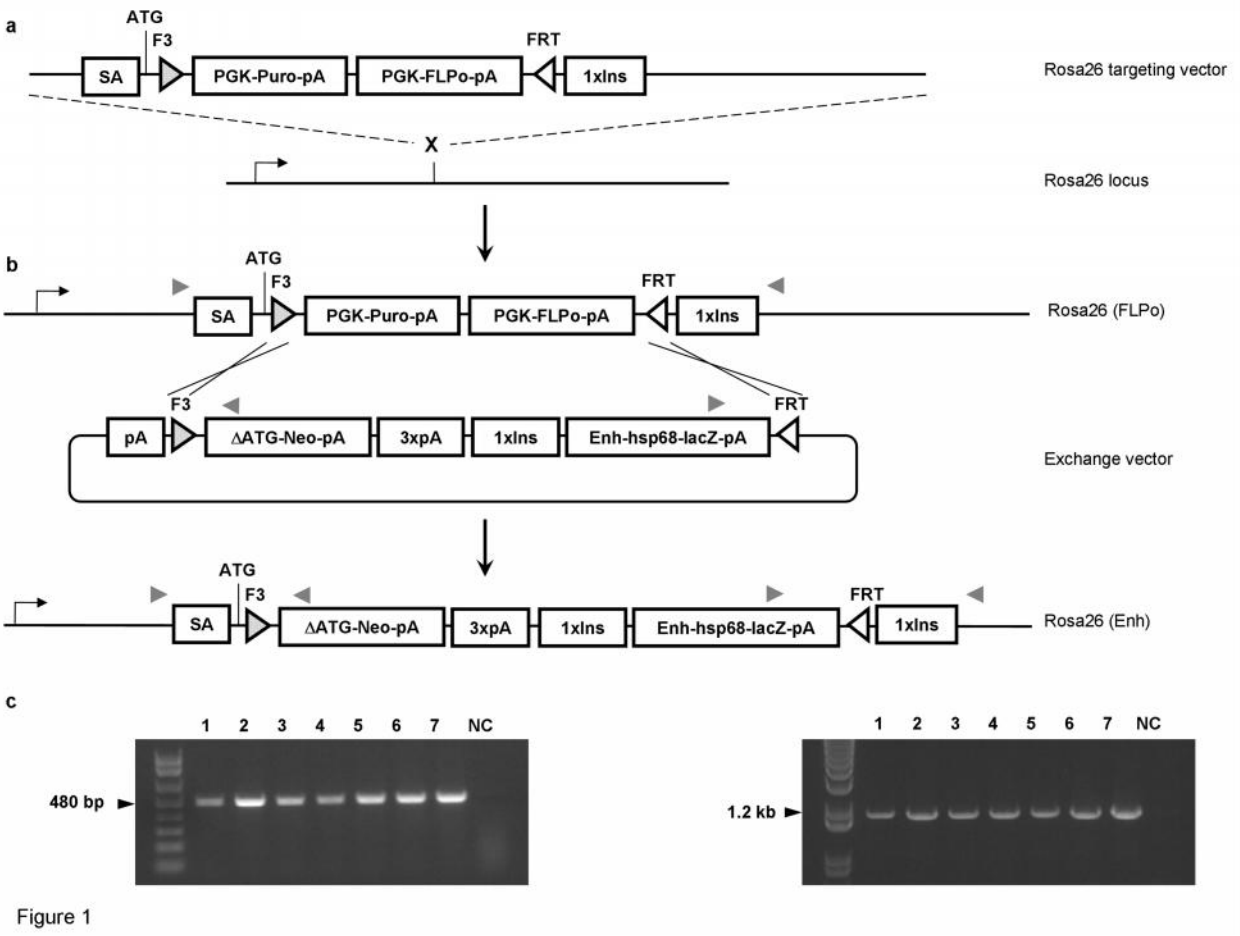
a
ATG
F3
FRT
SA
PGK-Puro-pA
PGK-FLPo-pA
1xIns
Rosa26 targeting vector
X
Rosa26 locus
b
ATG
F3
FRT
SA
PGK-Puro-pA
PGK-FLPo-pA
1xIns
Rosa26 (FLPo)
F3
FRT
pA
ΔATG-Neo-pA
3xpA
1xIns
Enh-hsp68-lacZ-pA
Exchange vector
ATG
F3
FRT
SA
ΔATG-Neo-pA
3xpA
1xIns
Enh-hsp68-lacZ-pA
1xIns
Rosa26 (Enh)
c
1 2 3 4 5 6 7 NC
480 bp
1 2 3 4 5 6 7 NC
1.2 kb

Figure 1

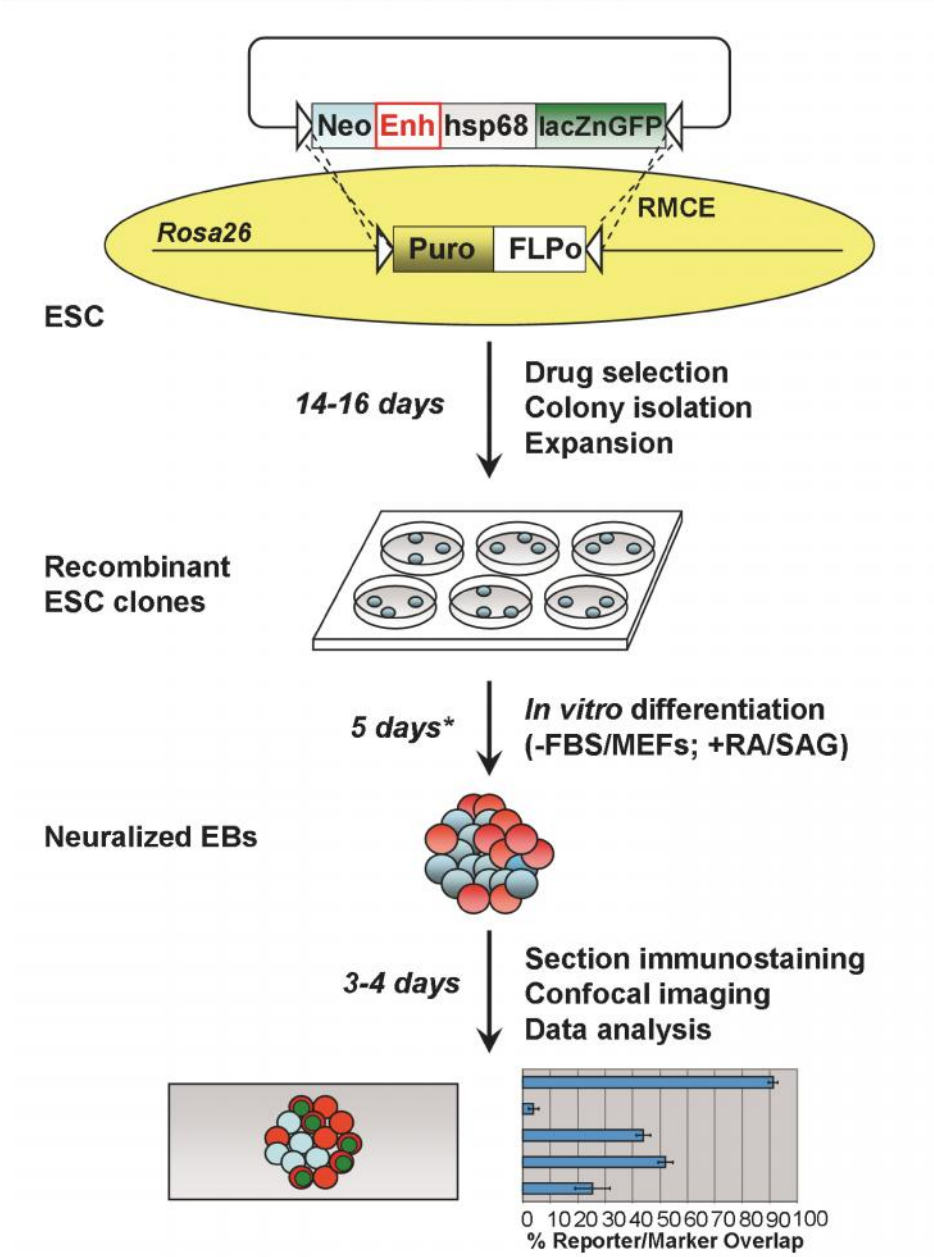
Neo
Enh
hsp68
lacZnGFP
Rosa26
Puro
FLPo
RMCE
ESC
14-16 days
Drug selection
Colony isolation
Expansion
Recombinant
ESC clones
5 days*
In vitro differentiation
(-FBS/MEFs; +RA/SAG)
Neuralized EBs
3-4 days
Section immunostaining
Confocal imaging
Data analysis
0 10 20 30 40 50 60 70 80 90 100
% Reporter/Marker Overlap

Figure 2

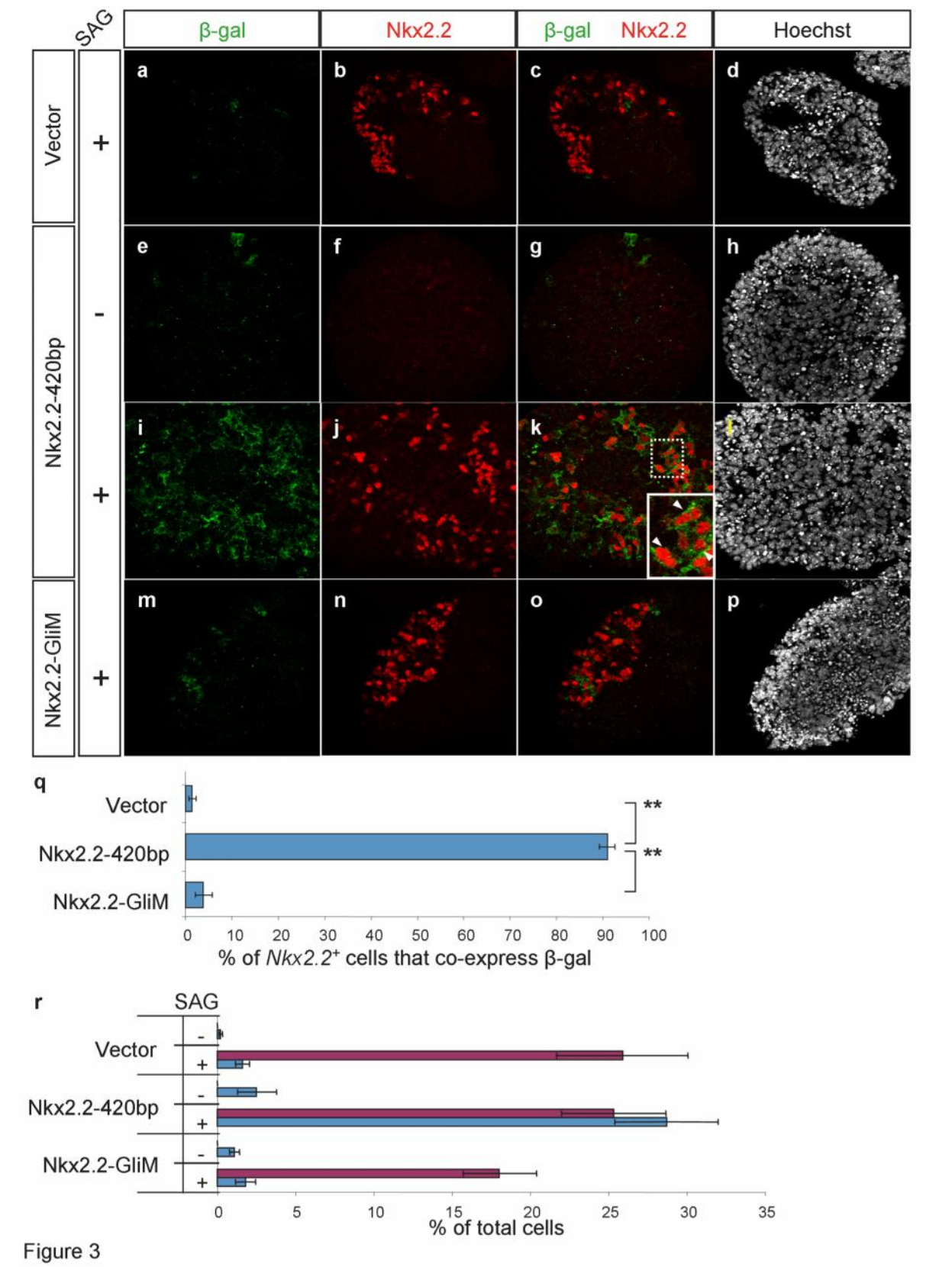
SAG
β-gal
Nkx2.2
β-gal Nkx2.2
Hoechst
Vector
Nkx2.2-420bp
Nkx2.2-GliM
+
-
+
+
a
b
c
d
e
f
g
h
i
j
k
l
m
n
o
p
q
Vector
Nkx2.2-420bp
Nkx2.2-GliM
**
**
0 10 20 30 40 50 60 70 80 90 100
% of Nkx2.2+ cells that co-express β-gal
r
SAG
Vector
Nkx2.2-420bp
Nkx2.2-GliM
-
+
-
+
-
+
0 5 10 15 20 25 30 35
% of total cells

Figure 3

Tables

Table 1. Summary of tested protocol modifications.

Protocol modification		**Number of recombinant colonies (per 10^6 electroporated cells)**
Number of electroporated cells ($x10^6$)	4.0	1.0* ± 0.1
	4.8	1.4* ± 0.3
	6.4	2.9 ± 0.1
Amount of electroporated DNA ($\mu g/10^6$ cells)	4.2	2.5
	8.3	1.7
	12.5	2.9
Exogenous FLPo	No	2.1* ± 0.5
	Yes	2.8* ± 0.7
Seeding cell density ($x10^5/cm^2$)	0.3	1.4* ± 0.3
	0.6	1.6* ± 0.1
	1.5	2.9* ± 1.7
	5.0	1.2* ± 0.2

*Average of at least three replicates.

Supplementary Figure Legend

Supplementary Figure 1. *Nkx2.2*-enhancer-driven expression of a nuclear reporter. Activity of the wild-type *Nkx2.2* enhancer (Nkx2.2-420bp) in the absence **(a-d)** or presence **(e-h)** of SAG; arrowheads in inset (g) point to *Nkx2.2*$^{+}$β-gal^{+} cells. Magnification: 40X.

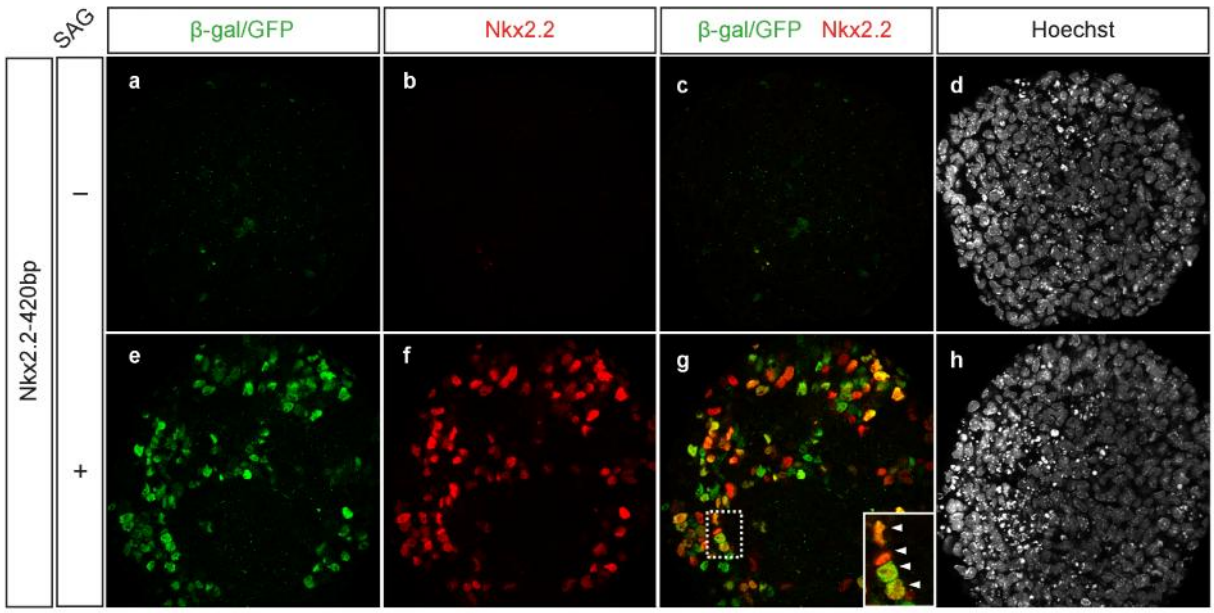

Supplementary Figure 1